

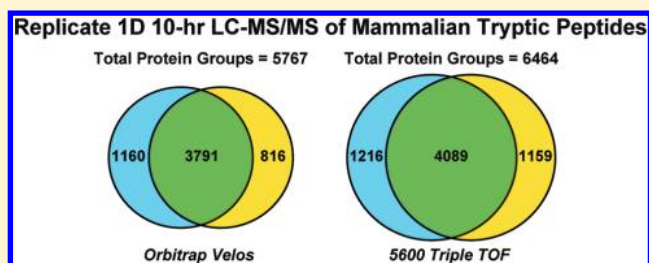
# Nanoflow Low Pressure High Peak Capacity Single Dimension LC-MS/MS Platform for High-Throughput, In-Depth Analysis of Mammalian Proteomes

Feng Zhou,<sup>‡</sup> Yu Lu,<sup>‡</sup> Scott B. Ficarro,<sup>†,‡</sup> James T. Webber,<sup>†</sup> and Jarrod A. Marto<sup>\*,†,‡</sup>

Department of Cancer Biology and <sup>†</sup>Blais Proteomics Center, Dana-Farber Cancer Institute, <sup>‡</sup>Department of Biological Chemistry and Molecular Pharmacology, Harvard Medical School, Boston, Massachusetts 02215-5450, United States

## Supporting Information

**ABSTRACT:** The use of narrow bore LC capillaries operated at ultralow flow rates coupled with mass spectrometry provides a desirable convergence of figures of merit to support high-performance LC-MS/MS analysis. This configuration provides a viable means to achieve in-depth protein sequence coverage while maintaining a high rate of data production. Here we explore potential performance improvements afforded by use of 25  $\mu\text{m} \times 100$  cm columns fabricated with 5  $\mu\text{m}$  diameter reversed phase particles and integrated electrospray emitter tips. These columns achieve a separation peak capacity of  $\approx 750$  in a 600-min gradient, with average chromatographic peak widths of less than 1 min. At room temperature, a pressure drop of only  $\approx 1500$  psi is sufficient to maintain an effluent flow rate of  $\leq 10$  nL/min. Using mouse embryonic stem cells as a model for complex mammalian proteomes, we reproducibly identify over 4000 proteins across duplicate 600 min LC-MS/MS analyses.



Improvements in chromatographic performance are an important component of efforts to achieve systematic and in depth proteome sequence analysis.<sup>1–5</sup> Pioneering work from multiple laboratories demonstrated the benefits of small particles ( $< 2 \mu\text{m}$ ),<sup>6–8</sup> ultranarrow bore columns ( $\leq 25 \mu\text{m}$  I.D.),<sup>9–11</sup> and high pressure solvent delivery (up to 70 000 psi).<sup>6</sup> Various combinations of these technologies have been used to attain single dimension separation peak capacity values of 700–1500.<sup>2,6,7,9,12–18</sup> As demonstrated originally by Novotny<sup>19,20</sup> and Jorgenson,<sup>21</sup> overall chromatographic performance improves with smaller diameter columns; in fact several variables converge to the benefit of electrospray performance under these circumstances. First, the volumetric flow at which optimal plate height is achieved varies with column inner diameter. Second, the effective analyte concentration, and hence signal intensity observed for LC-MS, increases approximately with the inverse square root of column inner diameter.<sup>9,22</sup> Finally, for aspect ratios (e.g., column diameter:particle diameter,  $d_c/d_p < 10$ ) obtained with small inner diameter ( $\leq 25 \mu\text{m}$ ), capillaries, and readily available reversed phase resins (3–5  $\mu\text{m}$  dia.), the column cross section is dominated by the loosely packed “wall region,” creating a more homogeneous packing structure.<sup>19–21,23,24</sup>

More recently, the commercial availability of columns packed with particles smaller than 2  $\mu\text{m}$  and ultrahigh pressure pump systems (UHPLC) have been widely used for mass spectrometry-based proteomics, typically with capillary columns of  $\geq 75 \mu\text{m}$  inner diameter.<sup>5,17</sup> The use of smaller particles at a fixed column I.D. maintains chromatographic resolution at increased flow rates, enabling so-called fast separations.<sup>6,25–27</sup>

However, recent work from our lab,<sup>28</sup> along with related studies,<sup>10,11,29–31</sup> has provided compelling evidence that the gains in electrospray ionization efficiency achieved at ultralow effluent flow rates more than compensate for diminished chromatographic performance. Moreover, multiple studies have suggested that the use of large particles packed in long beds is the best route to achieve maximum peak capacity for separation of complex mixtures.<sup>32–35</sup>

Collectively these data and observations suggest that a focus on smaller diameter capillaries packed with larger particles and operated in flow regimes below Van Deemter minima represents a promising path for improved LC-MS performance. Toward this end we fabricated 25  $\mu\text{m} \times 100$  cm columns with integrated electrospray emitters based on our previously described protocol.<sup>28</sup> Using mouse embryonic stem cells as a model for complex mammalian proteomes, we observed significant improvements in multiple analytical figures of merit for these extended length columns. Our data suggest that the use of narrow-bore capillaries packed with larger particles in extended bed lengths, and operation at ultralow flow rates provides a useful convergence of high peak capacity separation, high ionization efficiency, improved protein sequence analysis, and increased data production rate.

Received: November 25, 2011

Accepted: April 20, 2012

Published: April 21, 2012

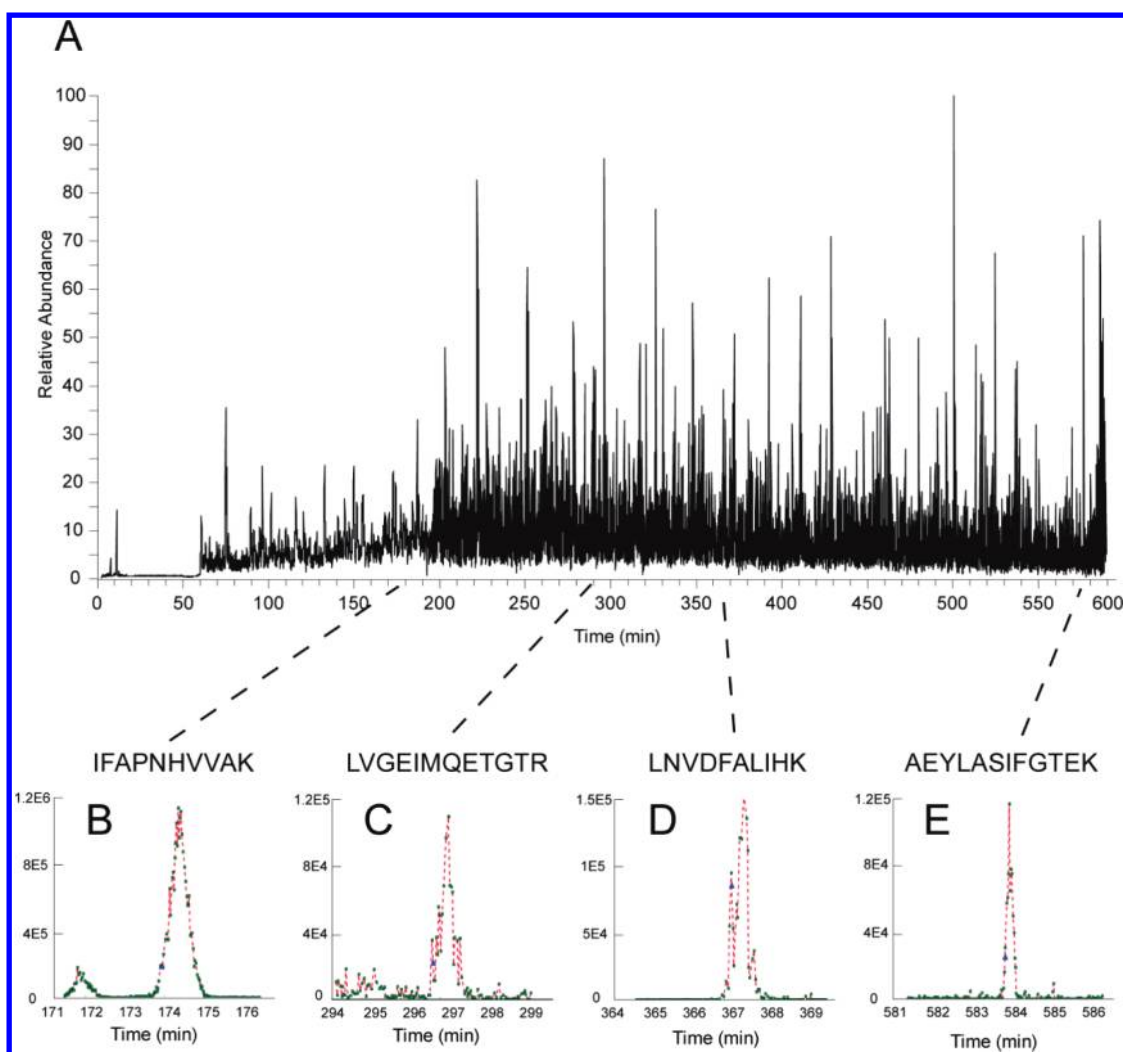


**Figure 1.** (A) Total ion chromatogram (TIC) for a 600 min gradient LC-MS/MS acquisition at a flow rate of 5 nL/min. (B–E) Representative extracted ion chromatograms (XIC) for peptides detected throughout the gradient: (B) IFAPNHVVAK; (C) LVGEIMQETGTR; (D) LNVDFALIHK; and (E) AEYLASIFGTEK.

## EXPERIMENTAL SECTION

Due to space considerations, experimental methods related to cell culture, sample preparation, and general mass spectrometry acquisition parameters are provided in the Supporting Information.

**Construction of 25  $\mu\text{m}$   $\times$  100 cm Fused Silica Analytical Columns with Integrated Emitter Tips.** The column packing procedure is similar to that described previously.<sup>28</sup> In brief, silicate-based frits were cast in situ as follows: A 2.5 cm section of polyimide was removed approximately 3 cm from one end of the fused silica tubing. A silicate solution was allowed to migrate via capillary action to four-fifths the length of the exposed window. Next, polymerization was induced using a soldering iron, with care taken to form frits of 1–2 mm in length. After ejection of excess silicate solution, the frits were reheated with the soldering iron at 400 °C for several seconds. Columns were slurry packed as previously described,<sup>28</sup> with 5  $\mu\text{m}$  diameter, 120 Å pore size Monitor C18 beads (Column Engineering, Ontario, CA) suspended in acetonitrile. Bed lengths of 100 cm were obtained after 48 h of continuous packing at  $\approx$ 1500 psi in a stainless steel vessel pressurized with helium. Next, the columns were dried with helium for 30 min. Finally, an integrated emitter tip of

0.75–1.5  $\mu\text{m}$  diameter was formed 2–4 mm beyond the frit using a laser-based pipet puller (P-2000, Sutter Instruments, Novato, CA). A 150  $\mu\text{m}$   $\times$  6 cm column packed with POROS 10R2 resin was prepared as previously described<sup>28</sup> and used as a precolumn (PC).

Our nanoflow LC platform was based on a Waters NanoACQUITY UHPLC system as described previously<sup>36</sup> and equipped with a 6-port, 2-position valve (VICI Valco, Houston, TX). We removed the first dimension column of the original 2D RP-RP configuration to create a one-dimension LC-MS/MS platform. The autosampler was used to load samples. True nanoflow rates in the analytical column were achieved through use of a passive flow split located prior to the reversed phase PC; the pre- and analytical-columns were configured in a vented geometry<sup>37,38</sup> as previously described.<sup>28</sup> We used two independent means to measure column flow rates. When the spray voltage was set  $>$ 5 kV bubbles form periodically in the column, and we estimated flow rate based on the time required to traverse a predefined segment of the capillary. The bubbles purge quickly once the spray voltage was reduced to normal operating levels ( $<$ 2.5 kV). Alternatively, we measured the displaced effluent volume by collection from the tip into an empty piece of 25 mm I.D. fused silica capillary, held

in place perpendicular to the emitter by a secondary clamp on the ESI source platform. Linear velocity was calculated based on parameters previously reported<sup>9</sup> for similar geometry LC assemblies.

**Data Analysis.** Our API-based multiplier<sup>39,40</sup> software framework was used to extract and format MS/MS data for subsequent search against an IPI mouse database v3.68. MS/MS data were searched using Protein Pilot V3.0 (AB Sciex, Foster City, CA) with the following parameters: instrument = "Orbitrap FT MS (sub-ppm), LTQ MS/MS" for data acquired from Orbitrap XL and Velos or "QSTAR Elite" for the 5600 Triple TOF. A fixed modification of +46 corresponding to methylthiolation of cysteine was also included. Only those peptides with scores at or above a FDR threshold of 1% were further considered. For the data herein, protein inference was based on this peptide set and performed in Protein Pilot V3.0, with identified proteins collapsed to protein groups. Comparisons to other data sets published on the mESC proteome were based only on peptides that mapped uniquely to gene IDs. Briefly, peptides passing the 1% FDR filter were classified as either "unique" or "shared" based on whether they could be assigned to only one or more than one gene ID, respectively.<sup>41,42</sup> Class 1 genes were defined as those identified only by unique peptides. Multiplierz scripts were used to systematically extract XICs and calculate corresponding peak widths for all identified peptides.

**Data Availability.** Lists of proteins and peptides associated with Figures 1, 3, and 4 are provided in Supporting Information files S1 and S2. In addition, all native mass spectrometry files are available for download from our Web site: <http://blaispathways.dfc.harvard.edu/mz/?id=doi:10.1021/ac2031404>

## SAFETY CONSIDERATIONS

Safety glasses should be worn at all times during construction and use of fused silica based capillaries. In addition, a lab coat and gloves should be worn when manipulating cell cultures in biosafety cabinets or when handling neat TFA and other volatile organics in a chemical fume hood.

## RESULTS AND DISCUSSION

We recently demonstrated the use of 25  $\mu\text{m} \times 10$  cm analytical columns<sup>28</sup> operated at true nanoflow regimes in online, automated 2D RP-RP<sup>36</sup> and 3D RP-SAX-RP<sup>43,44</sup> configurations for the analysis of complex proteomes. The latter system provided highly orthogonal separation between all three dimensions; based on these results we asked whether improved peak capacity in the final reversed phase stage would provide higher LC-MS/MS performance. Toward this end we extended the bed length of our analytical columns to 100 cm. In order to facilitate column packing and minimize the operating backpressure, we used 5  $\mu\text{m}$  diameter C18 resin. As noted by Ehlert et al.,<sup>23</sup> columns with a column-to-particle diameter ratio ( $d_c/d_p$ ) below  $\approx 10$  exhibit more homogeneous cross-sections dominated by loosely packed particles. Serendipitously, this configuration provides somewhat greater inter particle porosity, and hence, lower backpressure as compared to columns with closely packed ( $d_c/d_p > 10$ ) core regions.<sup>23</sup> We observed that a pressure drop of approximately 1400 psi across this column provided for an effluent flow rate of  $\approx 5$  nL/min at room temperature. This volumetric flow rate corresponds to a reduced velocity of  $\approx 0.021$  cm/s, or nearly an order of magnitude less than that determined for optimal chromato-

graphic peak width in similar slurry packed, microcapillary configurations.<sup>9</sup>

We first asked whether our 25  $\mu\text{m} \times 100$  cm columns would provide high peak capacity separation in the context of extended gradients. Toward this end, we analyzed tryptic peptides derived from murine embryonic stem cells (mESC). We chose these cells as they are reported to exhibit a greater degree of genomic stability as compared to typical immortalized tumor lines,<sup>45</sup> and hence may represent a suitable model system for platform performance comparisons across time and technologies. An aliquot corresponding to 200 ng of solubilized protein lysate was subjected to data-dependent LC-MS/MS on an Orbitrap XL in the context of a 10 h organic gradient. Figure 1A shows the total ion chromatogram (TIC) along with several extracted ion chromatograms (XIC) for peptides (panels B, C, D, and E) detected at various points throughout the gradient. Peak widths of less than 1 min were readily observed even near the end of the gradient (panel E). Next, we repeated this analysis on both 25  $\mu\text{m} \times 10$  cm and 25  $\mu\text{m} \times 100$  cm columns at various gradient lengths ranging from  $\approx 3$  to 10 h. For each LC-MS/MS acquisition, we calculated an average XIC peak width for all detected peptides within our multiplierz software environment<sup>39,40</sup> and plotted these as a function of gradient length (Figure 2A). We observed that the average peak width

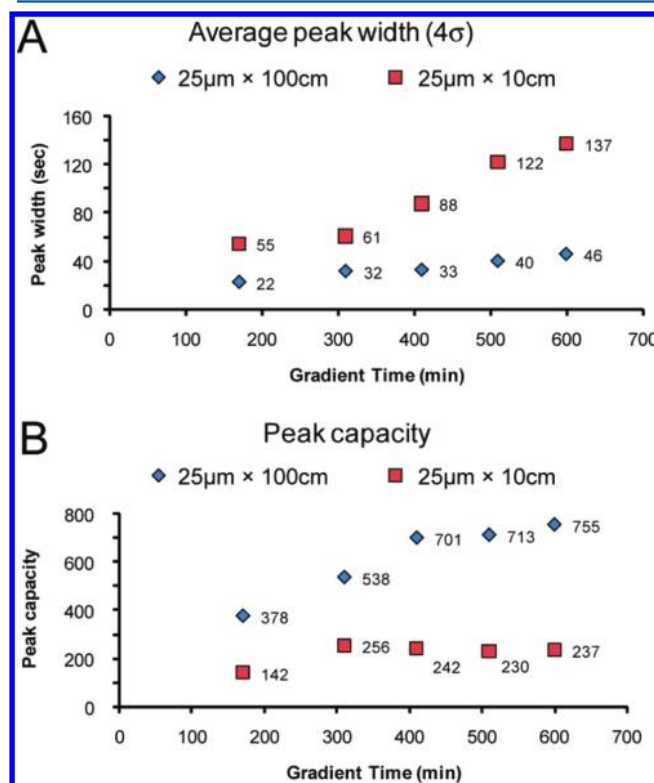


**Figure 2.** (A) Chromatographic peak width ( $4\sigma$ , where  $2\sigma$  is defined as fwhm of the corresponding XIC) and (B) separation peak capacity for (red) 25  $\mu\text{m} \times 10$  cm and (blue) 25  $\mu\text{m} \times 100$  cm columns as a function of LC gradient length. Peak capacity was estimated by dividing the time over which peptides were detected by the median peptide XIC peak width.

broadened rapidly as a function of gradient length for the 10 cm column while that for the 100 cm column remained less than 60 s, even for the longest gradient tested. On the basis of these data, we next calculated separation peak capacity and observed

that the  $25\ \mu\text{m} \times 100\ \text{cm}$  columns provided superior performance, reaching a maximum at  $\approx 750$  for a 10 h gradient (Figure 2B). Importantly the observed peak capacity for the 10 cm length columns was less than 50% of that for the extended length column and in fact diminished somewhat beyond a gradient length of  $\approx 300$  min. These results are consistent with previous reports suggesting that larger particles packed in extended length beds maximize separation peak capacity.<sup>32–35</sup>

To test whether the increased peak capacity translated into improved sequence coverage, we next plotted the number of unique peptides and proteins identified in these analyses (Figure 3A and B). In each case, the number of identifications mirrored the observed peak capacity, suggesting that separation quality was a major determinant of proteome sequence coverage as opposed to simply providing more time for exhaustive data-dependent MS/MS acquisition. In fact, at a gradient length of 600 min, the  $25\ \mu\text{m} \times 100\ \text{cm}$  analytical column provided a nearly 3-fold increase in the number of unique peptides identified as compared to the same analysis performed on the 10 cm column. We next increased the quantity of sample loaded to  $2\ \mu\text{g}$ , near the estimated upper limit of the  $150\ \mu\text{m} \times 4\ \text{cm}$  reversed phase precolumn assembly<sup>28</sup> and repeated the 10 h LC-MS/MS analysis; consistent with a previous report that systematically collated LC-MS/MS analytical figures of merit,<sup>46</sup> we observed an approximate 25% and 10% increase in the number of peptide and protein identifications, respectively (Figure 3A and B, rightmost bars). The rate of data production is also a useful metric to evaluate overall system efficiency. Toward this end, we plotted the numbers of peptides (Figure 3C) and protein groups (Figure 3D) identified per minute of LC-MS/MS acquisition time in the above experiments. The 100 cm long column exhibited remarkably stable efficiency across all conditions tested. Consistent with the reduced peak capacity observed as a function of gradient length with the  $25\ \mu\text{m} \times 10\ \text{cm}$  column, we also observed a concomitant drop in the rate of data production at longer gradients.

To explore further improvements afforded by a higher performance mass spectrometer, we next coupled the  $25\ \mu\text{m} \times 100\ \text{cm}$  column to a LTQ Velos Orbitrap instrument. In replicate, 10-h gradient acquisitions performed with  $2\ \mu\text{g}$  mESC whole cell lysate digests, we identified 4951 and 4607 protein groups, respectively (Figure 4A), and 5767 protein groups in total. The average data production rate across these two LC-MS/MS acquisitions was 45 and 9 peptide and protein identifications per minute, respectively. These data represent an approximate  $\approx 25\%$  improvement relative to those acquired on the Orbitrap XL platform. Given that we observed a 39% overlap in peptide sequences between replicate LC-MS/MS analyses (Figure 4A), we next systematically compared the relative retention times of the 200 most abundant peptides and found that they varied on average by 6% relative to the total acquisition time of 600 min. In addition we observed that some 80% of the corresponding precursor intensity ratios were within  $\pm 2$ -fold across replicate runs. It is conceivable that the convolution of peptide complexity in whole proteome digests, along with variation in retention time and the associated spray suppression effects, results in identification of different sequences across replicate LC-MS/MS acquisitions. To explore the possible contribution of stochastic precursor sampling during MS/MS, we repeated the 600 min gradient LC-MS experiments on an AB Sciex 5600 Triple TOF mass spectrometer, an instrument with improved MS/MS acquisition

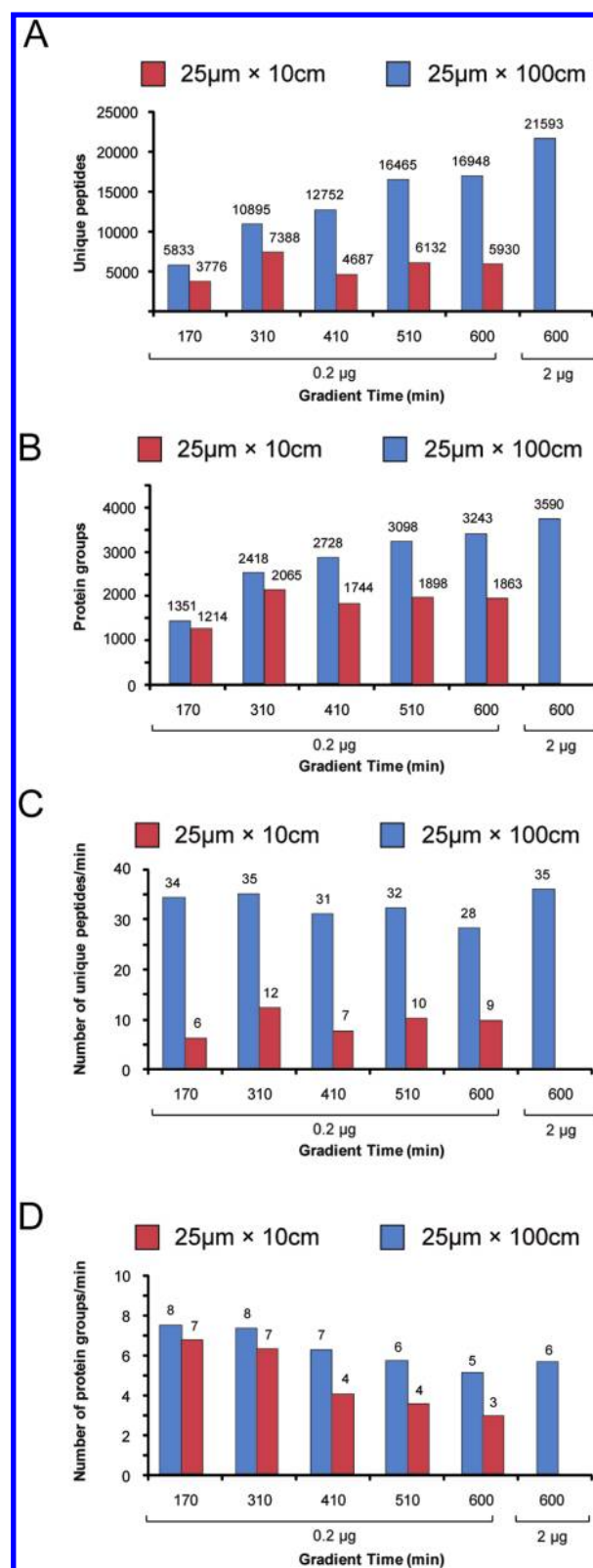


**Figure 3.** Number of (A) peptide and (B) protein group identifications as a function of gradient length and sample quantity for (red)  $25\ \mu\text{m} \times 10\ \text{cm}$  and (blue)  $25\ \mu\text{m} \times 100\ \text{cm}$  columns. Rate of (C) peptide and (D) protein group identifications per minute of LC-MS/MS acquisition time for (red)  $25\ \mu\text{m} \times 10\ \text{cm}$  and (blue)  $25\ \mu\text{m} \times 100\ \text{cm}$  columns.

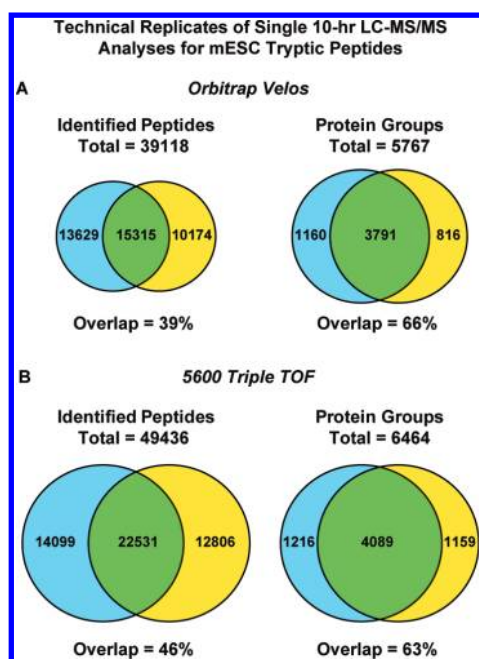


**Figure 4.** Venn diagrams representing the overlap of identified (left) peptides and (right) protein groups for technical replicate 600 min gradient LC-MS/MS analyses of tryptic peptides derived from mouse embryonic stem cells. (A) Data acquired from Thermo Fisher Velos Orbitrap. (B) Data acquired from AB Sciex 5600 TripleTOF.

rates. The reproducibility of sequence identification across replicate analyses increased to 46% (Figure 4B), while the average number of unique peptide and protein identifications increased by 32% and 10%, respectively, as compared to the Orbitrap Velos data. The average data production rate across these two LC-MS/MS acquisitions was 60 peptide and 9 protein identifications per minute, respectively. While the continued evolution of mass spectrometry instrumentation will undoubtedly provide broader proteome coverage independent of developments in LC technology,<sup>47–49</sup> detailed analyses have indicated that the incremental improvement provided by commercial advances in mass spectrometry hardware is somewhat offset by higher peak capacity separation.<sup>48</sup>

In general our data compare favorably in terms of sequence coverage and total acquisition time with a number of recent studies<sup>50–53</sup> that reported deep proteome analysis on the same mass spectrometry platform as described herein. For example, both the Mann<sup>54</sup> and Zeng<sup>55</sup> laboratories used an Orbitrap XL mass spectrometer in conjunction with SDS-PAGE gel and “Ying-Yang” pre-fractionation techniques, respectively, to analyze the mESC proteome. Using an independent script<sup>41,42</sup> on each of these data sets to identify those peptides that map to unique gene IDs, we found that our single, 10-hr acquisition on the Orbitrap XL compared favorably to these previous studies, identifying between 73–83% of the unique gene IDs (3487 genes in our data set versus 4789 and 4202 gene IDs from the Mann and Zeng datasets, respectively), in a fraction of the total LC-MS/MS acquisition time. Using the same gradient conditions on the Orbitrap Velos we identified an average of 4433 unique gene IDs across replicate analyses, within 5–10% of the above studies. Results from Köcher and colleagues,<sup>56</sup> based on LC-MS/MS analysis on an Orbitrap Velos of proteins derived from human cells, revealed similar trends as reported herein with respect to column and gradient length. In contrast to our column configuration (25  $\mu\text{m}$  I.D. packed with 5  $\mu\text{m}$

diameter beads) they opted for 75  $\mu\text{m}$  I.D. capillaries packed with 2  $\mu\text{m}$  diameter beads (25 and 50 cm bed lengths). Here again direct comparisons with our data are tempered by the experimental differences; however the large discrepancy between reported protein identifications, 2516 I.D.s (average value across triplicate measurements)<sup>56</sup> vs 3791 protein groups (reproduced across replicate measurements, Figure 4A) is consistent with the notion that smaller diameter columns packed with larger particles and operated at ultralow effluent flow rates maximizes LC-MS/MS data output.

Consistent with other recent reports,<sup>5,9,14,30,47,56–59</sup> our data support the idea that high-performance, single-dimension chromatography may provide a reasonable alternative to multidimensional fractionation in terms of the depth of proteome coverage and the total required acquisition time. In many cases, these systems are operated at ultrahigh pressure or elevated temperature. Open tubular<sup>11,29,31,60–62</sup> or monolithic stationary phases<sup>10,57,60,63</sup> have been successfully utilized as alternatives to slurry packed columns, although the overall binding capacity is often substantially less as compared to porous or semiporous<sup>64</sup> silica- or polymer-based particles. Similar to some of these recent reports, we also opted to use smaller diameter capillaries, but chose somewhat larger diameter reversed phase beads in order to simultaneously maintain high resolving power at low effluent flow rate, and hence optimal electrospray ionization efficiency,<sup>28</sup> along with a relatively low backpressure requirement of only  $\approx 1500$  psi. Indeed our 25  $\mu\text{m}$  I.D. column assemblies provided a peak capacity of  $\approx 750$  at a flow rate of  $\approx 5$  nL/min. (Figure 2B). This is approximately 50% of the total peak capacity reported by Shen, et al., for a 200 cm long column packed with 1.8  $\mu\text{m}$  particles and operated at a backpressure of nearly 20 000 psi.<sup>16</sup> Similarly, the peak capacity obtained on our 25  $\mu\text{m}$   $\times$  100 cm columns compares favorably to that obtained with 100  $\mu\text{m}$   $\times$  400 cm long monolithic C18 columns operated at  $\approx 6000$  psi.<sup>63</sup> Finally, as previously described,<sup>28</sup> our fabrication protocol is economical and requires no specialized equipment; in addition, the integrated electrospray emitters minimize deleterious band broadening often encountered when mechanical fittings are used to couple spray emitters with microcapillary columns. As with our 25  $\mu\text{m}$   $\times$  10 cm analytical columns, the extended length versions have proven very reliable and work is ongoing to integrate these with our fully automated 3D RP-SAX-RP<sup>43,44</sup> separation platform. Other interesting extensions of this work include using somewhat smaller particles (e.g.,  $\sim 3$   $\mu\text{m}$  dia.) in (i) the current 25  $\mu\text{m}$  I.D. capillaries to achieve higher throughput while maintaining relatively low backpressure (e.g.,  $< 5000$  psi.) or (ii) 15  $\mu\text{m}$  I.D. columns in order to maintain the same aspect ratio but utilize still lower effluent flow rates for potentially higher ionization efficiency during LC-MS/MS.

## CONCLUSIONS

Despite significant improvements in mass spectrometry performance,<sup>48,49,65</sup> obtaining in-depth sequence coverage for complex proteomes remains a difficult challenge. Moreover, the inherent limitations for parallel acquisition in mass spectrometry-based proteomics require that the depth of proteome coverage be considered within the context of data production rate and total instrument time. In this work, we describe the fabrication and relative performance improvements afforded by the use of 25  $\mu\text{m}$   $\times$  100 cm analytical columns packed with 5  $\mu\text{m}$  diameter reversed phase particles. These assemblies provide multiple figures of merit toward an optimal coupling of high

peak capacity separation and high efficiency electrospray ionization in LC-MS/MS. When used in conjunction with state-of-the-art mass spectrometry instrumentation, this 1D LC configuration simultaneously provides in-depth sequence coverage (average = 5277 protein groups across replicate analyses) and high data production rate (60 and 9 peptide and protein identifications per minute, respectively).

## ■ ASSOCIATED CONTENT

### ● Supporting Information

Supplementary experimental section. This material is available free of charge via the Internet at <http://pubs.acs.org>.

## ■ AUTHOR INFORMATION

### Corresponding Author

\*Mailing address: Department of Cancer Biology, Dana-Farber Cancer Institute, 450 Brookline Avenue, Smith 1158A, Boston, MA, 02215-5450, USA. Phone: (617) 632-3150. Fax: (617) 582-4471. E-mail: [jarrod\\_marto@dfci.harvard.edu](mailto:jarrod_marto@dfci.harvard.edu).

### Notes

The authors declare no competing financial interest.

## ■ ACKNOWLEDGMENTS

Generous support for this work was provided by the Dana-Farber Cancer Institute and the National Institutes of Health, NHGRI (P50HG004233), and NINDS (P01NS047572). The authors thank Karl Mechtler (IMP and IMBA, Vienna, Austria) for helpful suggestions and critical reading of our manuscript.

## ■ REFERENCES

- (1) Sandra, K.; Moshir, M.; D'Hondt, F.; Tuytten, R.; Verleysen, K.; Kas, K.; Francois, I.; Sandra, P. *J. Chromatogr. B* **2009**, *877*, 1019–1039.
- (2) De Villiers, A.; Cabooter, D.; Lynen, F.; Desmet, G.; Sandra, P. *J. Chromatogr. A* **2009**, *1216*, 3270–3279.
- (3) Slaughter, C.; High, A.; Galea, C.; Thomas, P.; Mishra, A.; Gebler, J.; Zhou, M.; Stine, M.; Finkelstein, D.; Obenauer, J.; Doherty, P.; Kriwacki, R. *Mol. Cell. Proteomics* **2007**, *6*, 46–46.
- (4) Michalski, A.; Cox, J.; Mann, M. *J. Proteome Res.* **2011**, *10*, 1785–1793.
- (5) Thakur, S. S.; Geiger, T.; Chatterjee, B.; Bandilla, P.; Frohlich, F.; Cox, J.; Mann, M. *Molec. Cell. Proteom.: MCP* **2011**, *10*, M110.003699.
- (6) MacNair, J. E.; Patel, K. D.; Jorgenson, J. W. *Anal. Chem.* **1999**, *71*, 700–708.
- (7) Patel, K. D.; Jerkovich, A. D.; Link, J. C.; Jorgenson, J. W. *Anal. Chem.* **2004**, *76*, 5777–5786.
- (8) Mellors, J. S.; Jorgenson, J. W. *Anal. Chem.* **2004**, *76*, 5441–50.
- (9) Shen, Y. F.; Zhao, R.; Berger, S. J.; Anderson, G. A.; Rodriguez, N.; Smith, R. D. *Anal. Chem.* **2002**, *74*, 4235–4249.
- (10) Wang, D. D.; Hincapie, M.; Rejtar, T.; Karger, B. L. *Anal. Chem.* **2011**, *83*, 2029–2037.
- (11) Yue, G. H.; Luo, Q. Z.; Zhang, J.; Wu, S. L.; Karger, B. L. *Anal. Chem.* **2007**, *79*, 938–946.
- (12) MacNair, J. E.; Lewis, K. C.; Jorgenson, J. W. *Anal. Chem.* **1997**, *69*, 983–989.
- (13) Shen, Y. F.; Tolic, N.; Zhao, R.; Pasa-Tolic, L.; Li, L. J.; Berger, S. J.; Harkewicz, R.; Anderson, G. A.; Belov, M. E.; Smith, R. D. *Anal. Chem.* **2001**, *73*, 3011–3021.
- (14) Shen, Y.; Tolic, N.; Masselon, C.; Pasa-Tolic, L.; Camp, D. G.; Hixson, K. K.; Zhao, R.; Anderson, G. A.; Smith, R. D. *Anal. Chem.* **2004**, *76*, 144–154.
- (15) Mazzeo, J. R.; Neue, U. D.; Kele, M.; Plumb, R. S. *Anal. Chem.* **2005**, *77*, 460A–467A.

- (16) Shen, Y. F.; Zhang, R.; Moore, R. J.; Kim, J.; Metz, T. O.; Hixson, K. K.; Zhao, R.; Livesay, E. A.; Udseth, H. R.; Smith, R. D. *Anal. Chem.* **2005**, *77*, 3090–3100.
- (17) Liu, H. J.; Finch, J. W.; Lavallee, M. J.; Collamati, R. A.; Benevides, C. C.; Gebler, J. C. *J. Chromatogr. A* **2007**, *1147*, 30–36.
- (18) Min, H. K.; Hyung, S. W.; Shin, J. W.; Nam, H. S.; Ahn, S. H.; Jung, H. J.; Lee, S. W. *Electrophoresis* **2007**, *28*, 1012–1021.
- (19) Karlsson, K. E.; Novotny, M. *Anal. Chem.* **1988**, *60*, 1662–1665.
- (20) Kennedy, R. T.; Jorgenson, J. W. *Anal. Chem.* **1989**, *61*, 1128–1135.
- (21) Hsieh, S. C.; Jorgenson, J. W. *Anal. Chem.* **1996**, *68*, 1212–1217.
- (22) Banks, J. F. *J. Chromatogr. A* **1996**, *743*, 99–104.
- (23) Ehlert, S.; Roesler, T.; Tallarek, U. *J. Sep. Sci.* **2008**, *31*, 1719–1728.
- (24) Knox, J. H.; Parcher, J. F. *Anal. Chem.* **1969**, *41*, 1599.
- (25) Castro-Perez, J.; Plumb, R.; Granger, J. H.; Beattie, I.; Joncour, K.; Wright, A. *Rapid Commun. Mass Spectr.: RCM* **2005**, *19*, 843–8.
- (26) MacNair, J. E.; Opitck, G. J.; Jorgenson, J. W.; Moseley, M. A., 3rd *Rapid Commun. Mass Spectr.: RCM* **1997**, *11*, 1279–85.
- (27) Tolley, L.; Jorgenson, J. W.; Moseley, M. A. *Anal. Chem.* **2001**, *73*, 2985–91.
- (28) Ficarro, S. B.; Zhang, Y.; Lu, Y.; Moghimi, A. R.; Askenazi, M.; Hyatt, E.; Smith, E. D.; Boyer, L.; Schlaeger, T. M.; Luckey, C. J.; Marto, J. A. *Anal. Chem.* **2009**, *81*, 3440–3447.
- (29) Ivanov, A. R.; Zang, L.; Karger, B. L. *Anal. Chem.* **2003**, *75*, 5306–5316.
- (30) Shen, Y. F.; Moore, R. J.; Zhao, R.; Blonder, J.; Auberry, D. L.; Masselon, C.; Pasa-Tolic, L.; Hixson, K. K.; Auberry, K. J.; Smith, R. D. *Anal. Chem.* **2003**, *75*, 3596–3605.
- (31) Luo, Q. Z.; Tang, K. Q.; Yang, F.; Elias, A.; Shen, Y. F.; Moore, R. J.; Zhao, R.; Hixson, K. K.; Rossie, S. S.; Smith, R. D. *J. Proteome Res.* **2006**, *5*, 1091–1097.
- (32) Wang, X. L.; Barber, W. E.; Carr, P. W. *J. Chromatogr. A* **2006**, *1107*, 139–151.
- (33) Poppe, H. *J. Chromatogr. A* **1997**, *778*, 3–21.
- (34) Scott, R. P. W.; Kucera, P. *J. Chromatogr.* **1979**, *169*, 51–72.
- (35) Wang, X. L.; Stoll, D. R.; Schellinger, A. P.; Carr, P. W. *Anal. Chem.* **2006**, *78*, 3406–3416.
- (36) Zhou, F.; Cardoza, J. D.; Ficarro, S. B.; Adelmant, G. O.; Lazaro, J. B.; Marto, J. A. *J. Proteome Res.* **2010**, *9*, 6242–6255.
- (37) van der Heeft, E.; ten Hove, G. J.; Herbets, C. A.; Meiring, H. D.; van Els, C.; de Jong, A. *Anal. Chem.* **1998**, *70*, 3742–3751.
- (38) Licklider, L. J.; Thoreen, C. C.; Peng, J. M.; Gygi, S. P. *Anal. Chem.* **2002**, *74*, 3076–3083.
- (39) Askenazi, M.; Parikh, J. R.; Marto, J. A. *Nat. Methods* **2009**, *6*, 240–242.
- (40) Parikh, J. R.; Askenazi, M.; Ficarro, S. B.; Cashorali, T.; Webber, J. T.; Blank, N. C.; Zhang, Y.; Marto, J. A. *BMC Bioinform.* **2009**, *10*, 364.
- (41) Grobei, M. A.; Qeli, E.; Brunner, E.; Rehrauer, H.; Zhang, R. X.; Roschitzki, B.; Basler, K.; Ahrens, C. H.; Grossniklaus, U. *Genome Res.* **2009**, *19*, 1786–1800.
- (42) Qeli, E.; Ahrens, C. H. *Nat. Biotechnol.* **2010**, *28*, 647–650.
- (43) Ficarro, S. B.; Zhang, Y.; Carrasco-Alfonso, M. J.; Garg, B.; Adelmant, G. O.; Webber, J. T.; Luckey, C. J.; Marto, J. A. *Mol. Cell. Proteomics* **2011**, *10*, O111.011064.
- (44) Zhou, F.; Sikorski, T. W.; Ficarro, S. B.; Webber, J. T.; Marto, J. A. *Anal. Chem.* **2011**, *83*, 6996–7005.
- (45) Zalzman, M.; Falco, G.; Sharova, L. V.; Nishiyama, A.; Thomas, M.; Lee, S. L.; Stagg, C. A.; Hoang, H. G.; Yang, H. T.; Indig, F. E.; Wersto, R. P.; Ko, M. S. H. *Nature* **2010**, *464*, 858–863.
- (46) Rudnick, P. A.; Clauser, K. R.; Kilpatrick, L. E.; Tchekhovskoi, D. V.; Neta, P.; Blonder, N.; Billheimer, D. D.; Blackman, R. K.; et al. *Mol. Cell. Proteomics* **2010**, *9*, 225–241.
- (47) Nagaraj, N.; Alexander Kulak, N.; Cox, J.; Neuhauser, N.; Mayr, K.; Hoerning, O.; Vorm, O.; Mann, M. *Mol. Cell. Proteomics* **2012**, *11*, M111.013722.

- (48) Second, T. P.; Blethrow, J. D.; Schwartz, J. C.; Merrihew, G. E.; MacCoss, M. J.; Swaney, D. L.; Russell, J. D.; Coon, J. J.; Zabrouskov, V. *Anal. Chem.* **2009**, *81*, 7757–7765.
- (49) Andrews, G. L.; Simons, B. L.; Young, J. B.; Hawkridge, A. M.; Muddiman, D. C. *Anal. Chem.* **2011**, *83*, 5442–5446.
- (50) de Godoy, L. M. F.; Olsen, J. V.; Cox, J.; Nielsen, M. L.; Hubner, N. C.; Frohlich, F.; Walther, T. C.; Mann, M. *Nature* **2008**, *455*, 1251–U60.
- (51) Baerenfaller, K.; Grossmann, J.; Grobei, M. A.; Hull, R.; Hirsch-Hoffmann, M.; Yalovsky, S.; Zimmermann, P.; Grossniklaus, U.; Gruissem, W.; Baginsky, S. *Science* **2008**, *320*, 938.
- (52) Beck, M.; Schmidt, A.; Malmstroem, J.; Claassen, M.; Ori, A.; Szymborska, A.; Herzog, F.; Rinner, O.; Ellenberg, J.; Aebersold, R. *Mol. Syst. Biol.* **2011**, *7*, 549.
- (53) Nagaraj, N.; Wisniewski, J. R.; Geiger, T.; Cox, J.; Kircher, M.; Kelso, J.; Paabo, S.; Mann, M. *Mol. Syst. Biol.* **2011**, *7*, 548.
- (54) Graumann, J.; Hubner, N. C.; Kim, J. B.; Ko, K.; Moser, M.; Kumar, C.; Cox, J.; Scholer, H.; Mann, M. *Mol. Cell. Proteomics* **2008**, *7*, 672–683.
- (55) Li, Q. R.; Xing, X. B.; Chen, T. T.; Li, R. X.; Dai, J.; Sheng, Q. H.; Xin, S. M.; Zhu, L. L.; Jin, Y.; Pei, G.; Kang, J. H.; Li, Y. X.; Zeng, R. *Mol. Cell. Proteomics* **2011**, *10*, M110.001750.
- (56) Kocher, T.; Swart, R.; Mechtler, K. *Anal. Chem.* **2011**, *83*, 2699–704.
- (57) Iwasaki, M.; Miwa, S.; Ikegami, T.; Tomita, M.; Tanaka, N.; Ishihama, Y. *Anal. Chem.* **2010**, *82*, 2616–2620.
- (58) Shen, Y. F.; Jacobs, J. M.; Camp, D. G.; Fang, R. H.; Moore, R. J.; Smith, R. D.; Xiao, W. Z.; Davis, R. W.; Tompkins, R. G. *Anal. Chem.* **2004**, *76*, 1134–1144.
- (59) Iwasaki, M.; Sugiyama, N.; Tanaka, N.; Ishihama, Y. *J. Chromatogr. A* **2012**, *1228*, 292–7.
- (60) Luo, Q. Z.; Shen, Y. F.; Hixson, K. K.; Zhao, R.; Yang, F.; Moore, R. J.; Mottaz, H. M.; Smith, R. D. *Anal. Chem.* **2005**, *77*, 5028–5035.
- (61) Luo, Q.; Page, J. S.; Tang, K. Q.; Smith, R. D. *Anal. Chem.* **2007**, *79*, 540–545.
- (62) Luo, Q.; Yue, G.; Valaskovic, G. A.; Gu, Y.; Wu, S. L.; Karger, B. L. *Anal. Chem.* **2007**, *79*, 6174–6181.
- (63) Eghbali, H.; Sandra, K.; Detobel, F.; Lynen, F.; Nakanishi, K.; Sandra, P.; Desmet, G. *J. Chromatogr. A* **2011**, *1218*, 3360–3366.
- (64) Gritti, F.; Cavazzini, A.; Marchetti, N.; Guiochon, G. *J. Chromatogr. A* **2007**, *1157*, 289–303.
- (65) Michalski, A.; Damoc, E.; Hauschild, J. P.; Lange, O.; Wieghaus, A.; Makarov, A.; Nagaraj, N.; Cox, J.; Mann, M.; Horning, S. *Mol. Cell. Proteomics* **2011**, *10*, M111.011015.